

Organization of Rigid Wedge–Flexible Coil Block Copolymers into Liquid Crystalline Assembly

Jinyoung Bae, Jung-Keun Kim, Nam-Keun Oh, and Myongsoo Lee*

Center for Supramolecular Nano-Assembly and Department of Chemistry, Yonsei University, Seoul 120-749, Korea

Received January 6, 2005; Revised Manuscript Received March 5, 2005

ABSTRACT: The synthesis and characterization of wedge–coil block molecules with a poly(ethylene oxide) coil of 77 (**1a**), 91 (**1b**), 114 (**1c**), and 182 (**1d**) ethylene oxide units are described. The self-assembling behavior of these block polymers in the melt state was investigated by optical polarized microscopy, differential scanning calorimetry (DSC), X-ray scattering measurements, and transmission electron microscopy (TEM). Block polymers self-organize from 1-D lamellar to 2-D hexagonal columnar liquid crystalline phases as the length of the PEO chain increases. This result demonstrates that supramolecular nanostructures can be controlled in a rigid wedge–flexible coil block copolymer system through introduction of a long flexible coil.

Introduction

The design of supramolecular architecture with well-defined shapes and size is of great importance to acquire desired properties for molecular materials.¹ Self-assembly of molecules through noncovalent forces including hydrophobic and hydrophilic effect, microphase segregation, and shape effects has the great potential for creating such supramolecular structures.² Among synthetic self-assembling molecular systems, rod–coil block molecules are of particular interest because of the potential of incorporating desirable chemical functionality and physical properties at nanoscale dimensions as well as many advantages associated with short chain lengths of the respective blocks.³ Dendritic molecular architecture is attractive building blocks to form such materials because they are well-defined in molecular architecture.⁴ The supramolecular structures can be precisely controlled by systematic variation of the type and relative length of the respective blocks.⁵

Combination of a rigid wedge-shaped building block into an amphiphilic block molecular architecture gives rise to a novel class of self-assembling systems because the molecule shares certain general characteristics of both dendrons and block copolymers.⁶ Recently, we have demonstrated that systematic variation in the coil length (PEO coil volume fraction, $f_{\text{PEO}} \leq 0.5$) can regulate the supramolecular structure, from 3-D micellar cubic with different lattices, 2-D hexagonal columnar, perforated lamellar to 1-D lamellar liquid crystalline assemblies.⁷ As an extension of this work, we have synthesized the wedge–coil block molecules with higher PEO coil volume fraction ($f_{\text{PEO}} > 0.5$) and investigated their supramolecular structure in the melt state.

The self-assembling behavior of these block polymers in the melt state was investigated by optical polarized microscopy, differential scanning calorimetry (DSC), X-ray scattering measurements, and transmission electron microscopy (TEM). These polymers were observed to self-assemble, as the length of the PEO chain increases, from a lamellar to a 2-D hexagonal columnar structure, in the melt state.

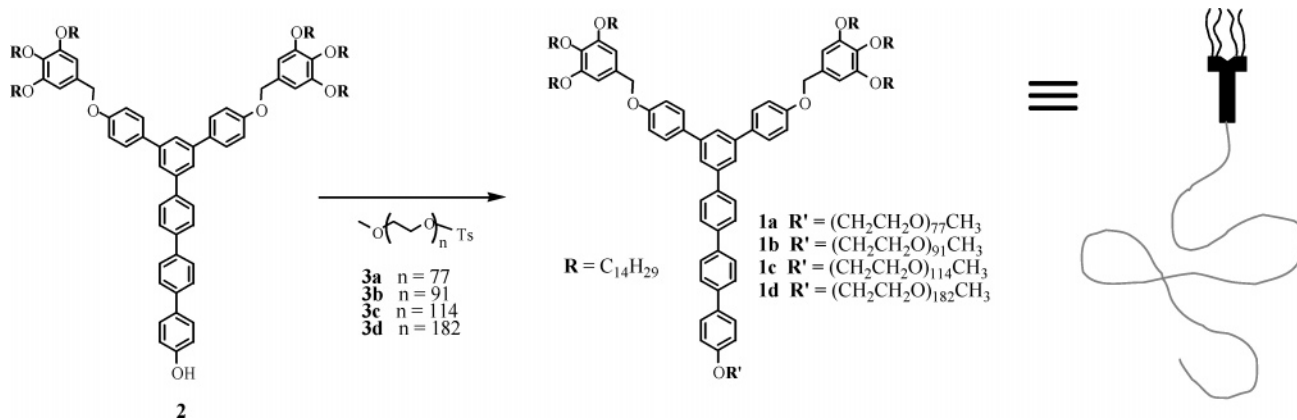
Experimental Section

Materials. NaH (60%), *p*-toluenesulfonyl chloride (98%) from Tokyo Kansei, and tetrakis(triphenylphosphine)palladium(0) (99%) from TCI were used as received. Poly(ethylene glycol) monomethyl ether ($\{\text{DP}\} = 114$), poly(ethylene oxide) ($\{\text{DP}\} = 77, 91, 182$), 4-bromo-4'-hydroxybiphenyl (99%), 1-bromotetradecane (98%), 1,3,5-tribromobenzene (99%), 4,4'-dibromobiphenyl (99%), *n*-butyllithium (1.6 M solution in *n*-hexane), 4-bromoanisole (99%), 4-bromobiphenyl (98%), borane–THF complex (1.0 M solution in THF), iodine monochloride (1.0 M solution in dichloromethane) (all from Aldrich), and the conventional reagents were used as received. 4-(*tert*-Butyldimethylsilyloxy)phenylboronic acid and 4-trimethylsilylbiphenyl-4'-boronic acid were prepared according to the similar procedures described previously. Unless otherwise indicated, all starting materials were obtained from commercial suppliers (Aldrich, Lancaster, TCI, etc.) All atmosphere-sensitive reactions were done under nitrogen. Visualization was accomplished with UV light and iodine vapor. Flash chromatography was carried out with silica gel 60 (230–400 mesh) from EM Science.

Techniques. ¹H and ¹³C NMR spectra were recorded from CDCl₃ and DMSO solutions on a Bruker AM 250 spectrometer. The purity of the products was checked by thin-layer chromatography (TLC; Merck, silica gel 60). A Perkin-Elmer DSC-7 differential scanning calorimeter equipped with 1020 thermal analysis controller was used to determine the thermal transitions, which were reported as the maxima and minima of their endothermic or exothermic peaks. In all cases, the heating and cooling rates were 10 °C min⁻¹. A Nikon Optiphot 2-pol optical polarized microscopy (magnification: 100×) equipped with a Mettler FP82 hot stage and a Mettler FP90 central processor was used to observe the thermal transitions and to analyze the anisotropic texture. Microanalysis was performed with a Perkin-Elmer 240 elemental analyzer at the Organic Chemistry Research Center. X-ray scattering measurements were performed in transmission mode with synchrotron radiation at the 3C2 X-ray beamline at Pohang Accelerator Laboratory, Korea. The molecular weight distribution (M_w/M_n) was determined by gel permeation chromatography (GPC) with a Waters R401 instrument equipped with Stragel HR 3, 4, and 4E columns, M7725i manual injector, column heating chamber, and 2010 Millennium data station. Measurements were made by using a UV detector, CHCl₃, as solvent (1.0 mL min⁻¹). MALDI-TOF-MS was performed on a Perceptive Biosystems Voyager-DE STR using a 2,5-dihydroxybenzoic acid matrix. Preparative high-performance liquid chromatography (HPLC) was performed at room temperature using a 20 mm × 600 mm polystyrene column on a Japan Analytical Industry model LC-

* To whom all correspondence should be addressed: Fax 82-2-393-6096; e-mail mslee@yonsei.ac.kr.

Scheme 1. Synthesis of the Wedge–Coil Block Copolymers 1a–d



908 recycling preparative HPLC system, equipped with a UV detector 310 and RI detector RI-5. The transmission electron microscope (TEM) was performed at 120 kV using a JEOL 1020. Ultrathin sectioning (ca. 50–70 nm thick) of specimens was performed by cryoultramicrotomy at -65°C using a RMC PowerTome-XL. Thin sections of specimen were transferred on a carbon-coated copper grid and stained with RuO_4 vapor.

Synthesis. A general outline of the synthetic procedure is shown in Scheme 1. The wedge–coil block copolymers were synthesized using a similar procedure described previously.^{7,8}

Synthesis of Compound 2. Compound 2 was synthesized using the same procedure described previously.

2: yield 44.6%. $^1\text{H NMR}$ (250 MHz, CDCl_3 , ppm): $\delta = 7.52$ – 7.77 (m, 17Ar–H), 7.12 (d, 4Ar–H; *o* to $-\text{OCH}_2\text{Ar}$, $J = 8.7$ Hz), 6.95 (d, 2Ar–H; *o* to OH, $J = 8.5$ Hz), 6.66 (s, 4Ar–H; *o* to $-\text{CH}_2\text{OAr}$), 5.01 (s, 4H, Ar CH_2OAr), 4.02 (t, 6H, $-\text{CH}_2\text{OAr}$), 1.26–1.83 (m, 144H, $-\text{CH}_2\text{CH}_2$), 0.90 (t, 18H, $-\text{CH}_2\text{CH}_3$). MALDI-TOF-MS m/z : 1982.53 ($[\text{M} + \text{Na}]^+$), calcd 1982.57.

Synthesis of Compounds 3a, 3b, 3c, and 3d. Compounds were synthesized using the same procedure. A representative example is described for compound 3a. Poly(ethylene oxide) monomethyl ether (5.0 g, 1.5 mmol) ($\{\text{DP}\} = 77$) and *p*-toluenesulfonyl chloride (0.8 g, 4.5 mmol) were dissolved in dry methylene chloride. Pyridine was added under nitrogen. The reaction mixture was stirred at 25°C under nitrogen for 5 h. The resulting solution was extracted with methylene chloride and washed with 1 M HCl and water. The methylene chloride solution was dried over anhydrous magnesium sulfate and filtered. The solvent was removed in a rotary evaporator, and the crude product was purified by column chromatography (silica gel) using ethyl acetate as eluent to yield 3.3 g (62%) of a colorless waxy solid.

3a: yield 62%. $^1\text{H NMR}$ (250 MHz, CDCl_3 , ppm): $\delta = 7.77$ (d, 2Ar–H; *o* to SO_3 , $J = 8.2$ Hz), 7.33 (d, 2Ar–H; *m* to SO_3 , $J = 8.0$ Hz), 4.14 (t, 2H, $-\text{CH}_2\text{OS}$), 3.51–3.67 (m, 302H, $-\text{CH}_2\text{O}$), 3.35 (s, 3H, CH_3O), 2.42 (s, 3H, CH_3 phenyl).

3b: yield 60%. $^1\text{H NMR}$ (250 MHz, CDCl_3 , ppm): $\delta = 7.77$ (d, 2Ar–H; *o* to SO_3 , $J = 8.2$ Hz), 7.33 (d, 2Ar–H; *m* to SO_3 , $J = 8.0$ Hz), 4.14 (t, 2H, $-\text{CH}_2\text{OS}$), 3.51–3.67 (m, 358H, $-\text{CH}_2\text{O}$), 3.35 (s, 3H, CH_3O), 2.42 (s, 3H, CH_3 phenyl).

3c: yield 64%. $^1\text{H NMR}$ (250 MHz, CDCl_3 , ppm): $\delta = 7.77$ (d, 2Ar–H; *o* to SO_3 , $J = 8.2$ Hz), 7.33 (d, 2Ar–H; *m* to SO_3 , $J = 8.0$ Hz), 4.14 (t, 2H, $-\text{CH}_2\text{OS}$), 3.51–3.67 (m, 450H, $-\text{CH}_2\text{O}$), 3.35 (s, 3H, CH_3O), 2.42 (s, 3H, CH_3 phenyl).

3d: yield 55%. $^1\text{H NMR}$ (250 MHz, CDCl_3 , ppm): $\delta = 7.77$ (d, 2Ar–H; *o* to SO_3 , $J = 8.2$ Hz), 7.33 (d, 2Ar–H; *m* to SO_3 , $J = 8.0$ Hz), 4.14 (t, 2H, $-\text{CH}_2\text{OS}$), 3.51–3.67 (m, 722H, $-\text{CH}_2\text{O}$), 3.35 (s, 3H, CH_3O), 2.42 (s, 3H, CH_3 phenyl).

Synthesis of Compounds 1a, 1b, 1c, and 1d. Compounds were synthesized using the same procedure. A representative example is described for compound 1a. Compound 2 (0.3 g, 0.47 mmol), compound 3a (3.3 g, 0.94 mmol), and excess K_2CO_3 were dissolved in 100 mL of DMF. The mixture was heated at reflux for 24 h. The resulting solution was poured into water and extracted with methylene chloride. The methylene chloride solution was washed with water, dried over

anhydrous magnesium sulfate, and filtered. Solvent was removed in a rotary evaporator. The reaction mixture was purified by column chromatography (silica gel) using ethyl acetate as eluent, and the crude product was further purified by recycle GPC to yield 1.6 g (61%) of a white solid.

1a: yield 61%. $^1\text{H NMR}$ (250 MHz, CDCl_3 , ppm): $\delta = 7.57$ – 7.76 (m, 17Ar–H), 7.12 (d, 4Ar–H; *o* to $-\text{OCH}_2\text{Ar}$, $J = 8.7$ Hz), 7.04 (d, 2Ar–H; *o* to OH, $J = 8.5$ Hz), 6.66 (s, 4Ar–H; *o* to $-\text{CH}_2\text{OAr}$), 5.01 (s, 4H, Ar CH_2OAr), 4.19 (t, 2H, $-\text{OCH}_2\text{CH}_2\text{OAr}$), 4.02 (m, 18H, $-\text{CH}_2\text{OAr}$), 3.51–3.96 (m, 300H, $-\text{CH}_2\text{O}$), 3.38 (s, 3H, CH_3O), 1.26–1.83 (m, 144H, $-\text{CH}_2\text{CH}_2$), 0.90 (t, 18H, $-\text{CH}_2\text{CH}_3$). Anal. Calcd for $\text{C}_{169}\text{H}_{276}\text{O}_{26}$: C, 64.73; H, 9.70. Found: C, 64.84; H, 9.94. MALDI-TOF-MS m/z 5403.21 ($[\text{M} + \text{Na}]^+$), calcd 5400.62.

1b: yield 55%. $^1\text{H NMR}$ (250 MHz, CDCl_3 , ppm): $\delta = 7.56$ – 7.77 (m, 17Ar–H), 7.11 (d, 4Ar–H; *o* to $-\text{OCH}_2\text{Ar}$, $J = 8.7$ Hz), 7.03 (d, 2Ar–H; *o* to OH, $J = 8.7$ Hz), 6.65 (s, 4Ar–H; *o* to $-\text{CH}_2\text{OAr}$), 5.01 (s, 4H, Ar CH_2OAr), 4.19 (t, 2H, $-\text{OCH}_2\text{CH}_2\text{OAr}$), 4.02 (m, 18H, $-\text{CH}_2\text{OAr}$), 3.51–3.96 (m, 356H, $-\text{CH}_2\text{O}$), 3.37 (s, 3H, CH_3O), 1.25–1.83 (m, 144H, $-\text{CH}_2\text{CH}_2$), 0.89 (t, 18H, $-\text{CH}_2\text{CH}_3$). Anal. Calcd for $\text{C}_{177}\text{H}_{292}\text{O}_{30}$: C, 63.63; H, 9.63. Found: C, 63.51; H, 9.77. MALDI-TOF-MS m/z 5999.56 ($[\text{M} + \text{Na}]^+$), calcd 6002.97.

1c: yield 59%. $^1\text{H NMR}$ (250 MHz, CDCl_3 , ppm): $\delta = 7.56$ – 7.77 (m, 17Ar–H), 7.11 (d, 4Ar–H; *o* to $-\text{OCH}_2\text{Ar}$, $J = 8.7$ Hz), 7.03 (d, 2Ar–H; *o* to OH, $J = 8.7$ Hz), 6.65 (s, 4Ar–H; *o* to $-\text{CH}_2\text{OAr}$), 5.01 (s, 4H, Ar CH_2OAr), 4.19 (t, 2H, $-\text{OCH}_2\text{CH}_2\text{OAr}$), 4.02 (m, 18H, $-\text{CH}_2\text{OAr}$), 3.51–3.96 (m, 448H, $-\text{CH}_2\text{O}$), 3.37 (s, 3H, CH_3O), 1.25–1.83 (m, 144H, $-\text{CH}_2\text{CH}_2$), 0.89 (t, 18H, $-\text{CH}_2\text{CH}_3$). Anal. Calcd for $\text{C}_{203}\text{H}_{344}\text{O}_{43}$: C, 62.36; H, 9.57. Found: C, 62.30; H, 9.66. MALDI-TOF-MS m/z 7027.92 ($[\text{M} + \text{Na}]^+$), calcd 7029.59.

1d: yield 51%. $^1\text{H NMR}$ (250 MHz, CDCl_3 , ppm): $\delta = 7.56$ – 7.77 (m, 17Ar–H), 7.11 (d, 4Ar–H; *o* to $-\text{OCH}_2\text{Ar}$, $J = 8.7$ Hz), 7.03 (d, 2Ar–H; *o* to OH, $J = 8.7$ Hz), 6.65 (s, 4Ar–H; *o* to $-\text{CH}_2\text{OAr}$), 5.01 (s, 4H, Ar CH_2OAr), 4.19 (t, 2H, $-\text{OCH}_2\text{CH}_2\text{OAr}$), 4.02 (m, 18H, $-\text{CH}_2\text{OAr}$), 3.51–3.96 (m, 720H, $-\text{CH}_2\text{O}$), 3.37 (s, 3H, CH_3O), 1.25–1.83 (m, 144H, $-\text{CH}_2\text{CH}_2$), 0.89 (t, 18H, $-\text{CH}_2\text{CH}_3$). Anal. Calcd for $\text{C}_{225}\text{H}_{388}\text{O}_{54}$: C, 60.01; H, 9.45. Found: C, 59.66; H, 9.62. MALDI-TOF-MS m/z 10024.03 ($[\text{M} + \text{Na}]^+$), calcd 10023.37.

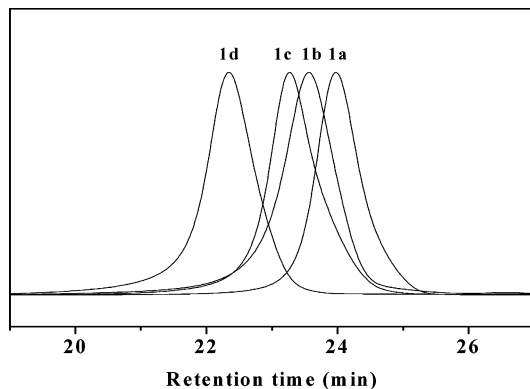
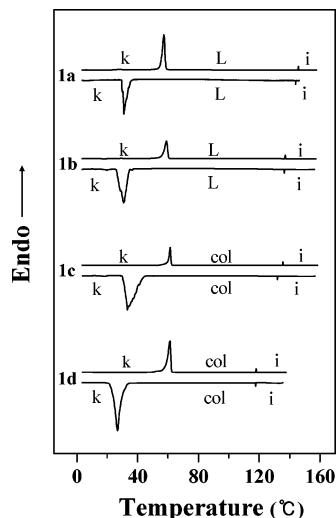
Results and Discussion

The synthesis of rigid wedge–flexible coil block copolymers (**1a**, **1b**, **1c**, and **1d**) consisting of a wedge-shaped rigid aromatic segment containing a tetradecyloxy periphery and a flexible PEO chain started with the preparation of an aromatic scaffold with a tetradecyloxy periphery according to the procedures described previously.⁷ The final wedge–coil block polymers were synthesized by an etherification reaction of a phenolic precursor with the appropriate tosyl-terminated PEO chains, as shown in Scheme 1.

Table 1. Thermal Transitions of 1a–d Molecules (Data Are from Heating and Cooling Scans)

molecules	coil DP	M_w/M_n^b	phase transition (°C) and corresponding enthalpy changes (kJ/mol) ^a					
			heating		cooling			
1a	77	1.03	k 57.3 (97.8)	L 145.6 (0.12)	i	i 143.6 (0.10)	L 23.3 (89.6)	k
1b	91	1.05	k 59.0 (80.5)	L 137.01 (0.03)	i	i 136.3 (0.04)	L 30.7 (76.1)	k
1c	114	1.06	k 61.5 (114.9)	col 134.8 (0.04)	i	i 131.0 (0.02)	col 33.3 (112.0)	k
1d	182	1.04	k 61.4 (131.6)	col 117.6.0 (0.29)	i	i 117.2 (0.26)	col 26.1 (119.2)	k

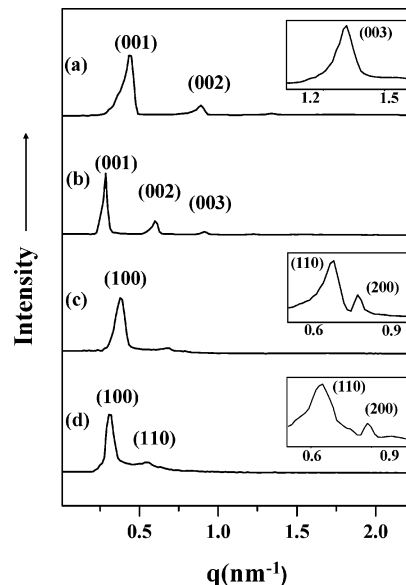
^a k: crystalline; i: isotropic; L: lamellar; col: hexagonal columnar. ^b Determined by GPC.

**Figure 1.** GPC traces of **1a–d**.**Figure 2.** DSC traces (10 °C/min) of block copolymers **1a–d** recorded during the heating and the cooling scan (k: crystalline phase; col: hexagonal columnar phase; L: lamellar phase; i: isotropic phase).

The resulting block polymers were purified by silica gel column chromatography using ethyl acetate as an eluent and then further purified by preparative gel permeation chromatography (prep. GPC) as described in the Experimental Section. The resulting polymers were characterized by NMR spectroscopy, elemental analysis, and MALDI-TOF mass spectroscopy and shown to be in full agreement with the structures presented.

Figure 1 shows GPC traces of polymers. As shown in Table 1, the polydispersity of the polymers measured by gel permeation chromatography (GPC) with the use of polystyrene standards appeared to be less than 1.06.

The self-assembling behavior of the block copolymers was investigated by differential scanning calorimetry (DSC), thermal polarized optical microscopy (POM), small- and wide-angle X-ray scatterings (SAXS and WAXS), and transmission electron microscopy (TEM). Figure 2 shows the DSC heating and cooling scans of the block copolymers. The thermal transition temper-

**Figure 3.** Small-angle X-ray diffraction patterns of **1a–d** plotted against q . (a) The lamellar lattice exhibited by **1a** at 100 °C, (b) the lamellar lattice exhibited by **1b** at 80 °C, (c) the hexagonal columnar lattice exhibited by **1c** at 80 °C, and (d) the hexagonal columnar lattice exhibited by **1d** at 100 °C.**Table 2. Characterization of 1a–d by Small-Angle X-ray Scattering**

molecules	f_{PEO}^a	calcd molecular length (nm)	liquid crystalline phase	
			lamellar phase d (nm)	hexagonal columnar phase d_{100} (nm) a (nm)
1a	0.63	27.0	14.3	
1b	0.67	31.2	17.3	
1c	0.72	38.1		16.5 19.1
1d	0.81	58.5		20.3 23.5

^a f_{PEO} = volume fraction of PEO group to hydrophilic part.

atures and corresponding enthalpy changes are summarized in Table 1.

As shown in Figure 2, all of the block copolymers exhibit thermotropic liquid crystalline phases. The wide-angle X-ray diffraction patterns in the melt state of all the polymers are characterized by a diffuse scattering, confirming the liquid crystalline nature. However, a supramolecular structural variation in the melt state was observed as the length of the PEO segment is varied, as evidenced by optical microscopic textures and small-angle X-ray scatterings (SAXS).

Optical microscopic images of **1a** and **1b** showed a focal conic texture in the melt state, indicative of the formation of a smectic A phase. The small-angle X-ray diffraction patterns display three reflections in the 1:2:3 spacing ratio, characteristic of a lamellar lattice (Figure 3a,b). The layer thickness obtained from the X-ray diffraction pattern appeared to be 14.3 and 17.3 nm for **1a** and **1b**, respectively, which are much smaller than

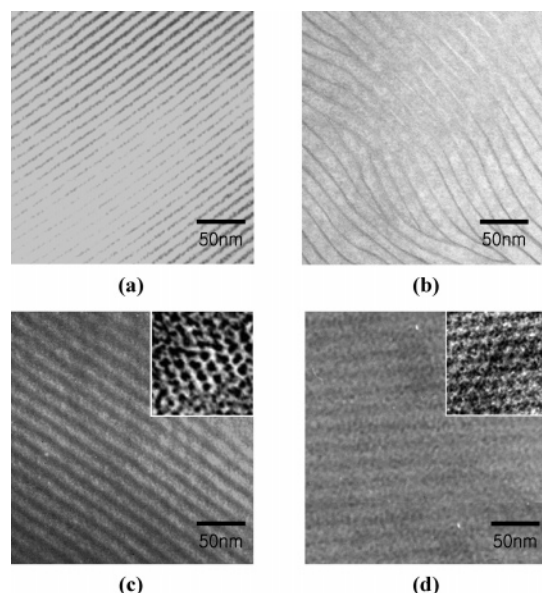


Figure 4. Representative TEM images of (a, b) an ultra-microtomed film of **1a** and **1b** stained with RuO_4 revealing layer ordered array of alternating light PEO layers and dark aromatic layers; (c, d) an ultra-microtomed film of **1c** and **1d** stained with RuO_4 exhibiting alternating dark rod layers and light PEO layers. The inset of the right provides in-plane hexagonally ordered array of dark rod segments.

the estimated molecular lengths (Table 2). This phase identification is further confirmed by TEM experiments (stained with RuO_4) that show organized dark, stained 1-D aromatic layers with a thickness of 3 nm (Figure 4a,b). Considering the molecular length and aromatic rod length (3 nm by Corey–Pauling–Koltun (CPK) molecular model), the dark aromatic domains in the image suggest that the molecules are packed with a

monolayer lamellar structure in which the rigid wedge segments are fully interdigitated, as shown in Figure 5a.

In contrast to those of **1a** and **1b**, the small-angle X-ray diffraction patterns for **1c** and **1d** in the liquid crystalline phase display three reflections of a 1: $\sqrt{3}$: $\sqrt{4}$ (Figure 3c,d), characteristic of a 2-D hexagonal columnar structure. From the observed first-order reflections, the lattice constants can be estimated to be 19.1 and 23.5 nm for **1c** and **1d**, respectively (Table 2). This phase identification is further supported by POM and TEM observations. On cooling from the isotropic liquid, a pseudo-focal conic texture was observed on optical polarized microscope, supporting the formation of a 2-D hexagonal columnar structure.⁹ The TEM images stained with RuO_4 showed a hexagonally array of dark spots in a matrix of light PEO chains as well as views in the column direction (Figure 4c,d). The more stained aromatic domains in the images showed the much thicker compared to those of the lamellar structure. Indeed, the columnar thickness obtained from TEM was measured to be 5.5 nm, which is similar to the estimated length of rigid wedge together with tetradecyl groups (5.5 nm by CPK). These results suggest that **1c** and **1d** self-assemble into a 2-D hexagonal columnar structure in which the hydrophobic segments consisting of a rigid wedge and tetradecyl groups are fully interdigitated with each other, as shown in Figure 5b. This result indicates that increasing coil length leads to transformation of a monolayer lamellar structure to a 2D-hexagonally columnar structure in which inner core consists of a rigid wedge and tetradecyl chains.

The results described above demonstrate the capability of manipulating the supramolecular structure based on same wedge-shaped rigid building block by grafting

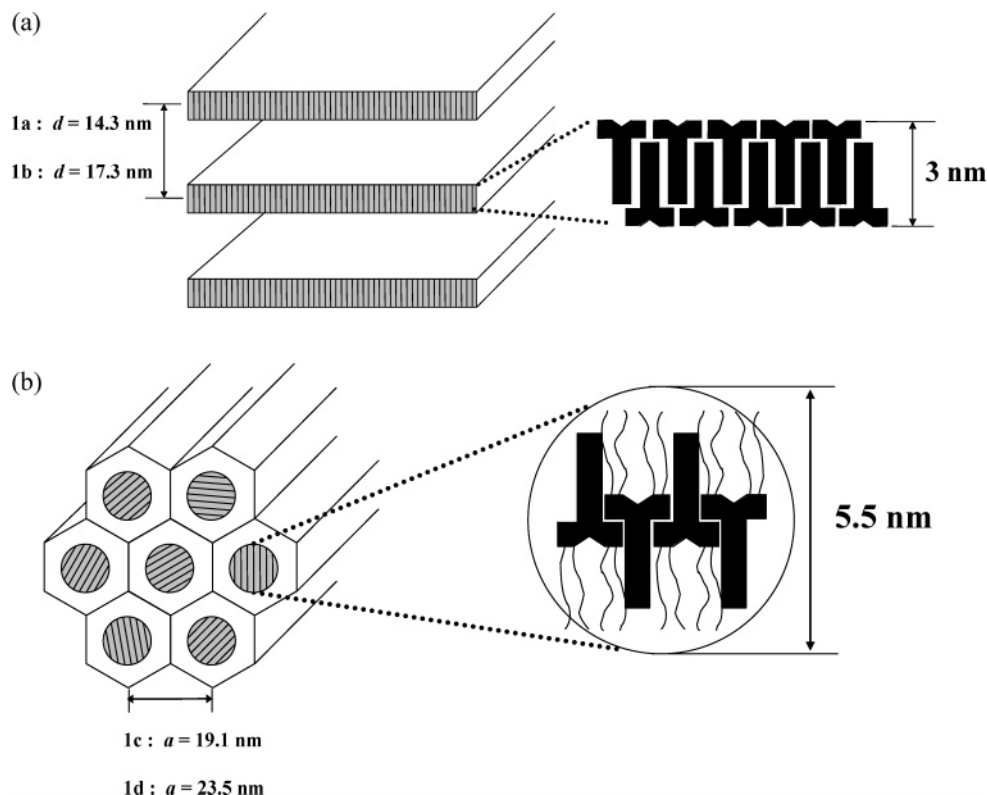


Figure 5. Schematic representation for (a) the lamellar structure of **1a** and **1b** and (b) the hexagonal columnar structure of **1c** and **1d**.

flexible PEO chains of different lengths. The tendency of a 1D-lamellar phase to transform into a 2D-hexagonal columnar phase is consistent with the results from rod-coil systems described previously.¹⁰ The variation of supramolecular structure can be rationalized by considering the microphase separation between the dissimilar parts of the molecule and the space-filling requirement of flexible PEO chains.¹¹ The molecules with a medium length of PEO chain would pack with a parallel arrangement with interdigitation of rigid aromatic segments to produce a flat interface as in the case of **1a** and **1b**.

However, increasing the length of the PEO chain results in more space for the hydrophilic chains being required while maintaining a constant density of the hydrophobic domains. Consequently, the sheetlike rod layers will break up into 2-D cylindrical domains in which less confinement and deformation of PEO chains occur, in which wedge-shaped aromatic segments and tetradecyl chains are mixed together within a domain. It is worthy of note that the 2-D hexagonal columnar structure obtained from the homologue based on a short PEO coil ($f_{\text{PEO}} = 0.32$) was proposed to consist of phase-separated three subdomains with a radial arrangement of the rigid blocks.⁷ Although the existence of a hexagonal columnar structure has also been reported in rigid aromatic-flexible dendritic molecules, it was proposed to consist of three subdomains with a parallel arrangement of the rigid blocks.^{8a} In addition, dendron-rod-dendron triblock molecules have been observed to self-assemble into a similar hexagonal columnar structure. However, the rod segments within a domain in these molecules were proposed to pack with antiparallel bundlelike arrangements that are perpendicular to each other in consecutive arrays.^{6a}

The self-organization phenomena of the series of rigid wedge-flexible coil block polymers demonstrate that systematic variation in the coil length can regulate the supramolecular structure, from lamellar to 2-D hexagonal columnar liquid crystalline assemblies. The primary force responsible for this structural change is believed to be the combination of shape complementarity and microphase separation between hydrophobic rigid-hydrophilic flexible segments. This result suggests that our approach of controlling supramolecular structures using rigid wedge molecules can lead to the construction of a variety of well-defined nanostructures.

Acknowledgment. This work was supported by the Creative Research Initiative Program of the Ministry

of Science and Technology, Korea, and Pohang Accelerator Laboratory, Korea (for using synchrotron radiation).

References and Notes

- (1) (a) Lehn, J. M. *Supramolecular Chemistry, Concepts and Perspectives*; VCH: Weinheim, Germany, 1995. (b) Lee, M.; Cho, B.-K.; Zin, W.-C. *Chem. Rev.* **2001**, *101*, 3869–3892. (c) Elemans, J. A. A. W.; Rowan, A. E.; Nolte, R. J. M. *J. Mater. Chem.* **2003**, *13*, 2661–2670. (d) Muthukumar, M.; Ober, C. K.; Thomas, E. L. *Science* **1997**, *277*, 1225–1232.
- (2) (a) Förster, S.; Plantenberg, T. *Angew. Chem., Int. Ed.* **2002**, *41*, 688–714. (b) Förster, S.; Antonietti, M. *Adv. Mater.* **1998**, *10*, 195–217.
- (3) (a) Lee, M.; Yoo, Y.-S. *J. Mater. Chem.* **2002**, *12*, 2161–2168. (b) Klok, H.-A.; Lecommandoux, S. *Adv. Mater.* **2001**, *13*, 1217–1229.
- (4) (a) Grayson, S. M.; Fréchet, J. M. J. *Chem. Rev.* **2001**, *101*, 3819–3868. (b) Moore, J. S. *Acc. Chem. Res.* **1997**, *30*, 402–413. (c) Percec, V.; Ahn, C.-H.; Ungar, G.; Yeardley, D. J. P.; Möller, M.; Sheiko, S. S. *Nature (London)* **1998**, *391*, 161–164. (d) Zeng, F.; Zimmerman, S. C. *Chem. Rev.* **1997**, *97*, 1681–1712. (e) Schenning, A. P. H. J.; Elissen-Roman, C.; Weener, J. W.; Baars, M. W. P. L.; van der Gaast, S. J.; Meijer, E. W. *J. Am. Chem. Soc.* **1998**, *120*, 8199–8208.
- (5) (a) Lee, M.; Cho, B.-K.; Kim, H.; Yoon, J.-Y.; Zin, W.-C. *J. Am. Chem. Soc.* **1998**, *120*, 9168–9179. (b) Lee, M.; Cho, B.-K.; Oh, N.-K.; Zin, W.-C. *Macromolecules* **2001**, *34*, 1987–1995. (c) Lee, M.; Cho, B.-K.; Ihn, K. J.; Lee, W.-K.; Oh, N.-K.; Zin, W.-C. *J. Am. Chem. Soc.* **2001**, *123*, 4647–4648. (d) Ryu, J.-H.; Oh, N.-K.; Zin, W.-C.; Lee, M. *J. Am. Chem. Soc.* **2004**, *126*, 3551–3558.
- (6) (a) Lecommandoux, S.; Klok, H.-A.; Sayar, M.; Stupp, S. I. *J. Polym. Sci., Polym. Chem.* **2003**, *41*, 3501–3518. (b) Tian, L.; Yam, L.; Zhou, N.; Tat, H.; Urich, K. E. *Macromolecules* **2004**, *37*, 538–543. (c) Johnson, M. A.; Iyer, J.; Hammond, P. T. *Macromolecules* **2004**, *37*, 2490–2501. (d) Cho, B.-K.; Jain, A.; Nieberle, J.; Mahajan, S.; Gruner, S. M.; Türk, S.; Räder, H. J. *Macromolecules* **2004**, *37*, 4227–4234.
- (7) Kim, J.-K.; Hong, M.-K.; Ahn, J.-H.; Lee, M. *Angew. Chem., Int. Ed.* **2005**, *44*, 328–332.
- (8) (a) Jang, C.-J.; Ryu, J.-H.; Lee, J.-D.; Sohn, D.; Lee, M. *Chem. Mater.* **2004**, *16*, 4226–4231. (b) Yoo, Y.-S.; Choi, J.-H.; Song, J.-H.; Oh, N.-K.; Zin, W.-C.; Park, S.; Chang, T.; Lee, M. *J. Am. Chem. Soc.* **2004**, *126*, 6294–6300.
- (9) Plasseraud, L.; Cuervo, L. G.; Guillon, D.; Süß-Fink, G.; Deschenaux, R.; Bruce, D. W.; Donnio, B. *J. Mater. Chem.* **2002**, *12*, 2653–2658.
- (10) (a) L. H. Radzilowski, S. I. Stupp. *Macromolecules* **1994**, *27*, 7747–7753. (b) Reenders, M.; ten Brinke, G. *Macromolecules* **2002**, *35*, 3266–3280. (c) Rueff, J.-M.; Barbera, J.; Donnio, B.; Guillon, D.; Marcos, M.; Serrano, J.-L. *Macromolecules* **2003**, *36*, 8368–8375. (d) Li, C. Y.; Tennesi, K. K.; Zhang, D.; Zhang, H.; Wan, X.; Chen, E.-Q.; Zhou, Q.-F.; Carlos, A.-O.; Igos, S.; Hsiao, B. S. *Macromolecules* **2004**, *37*, 2854–2860.
- (11) Williams, D. R. M.; Fredrickson, G. H. *Macromolecules* **1992**, *25*, 3561–3568.

MA0500281